BBA - Molecular Basis of Disease 1865 (2019) 1341–1350

Contents lists available at ScienceDirect

BBA - Molecular Basis of Disease

journal homepage: www.elsevier.com/locate/bbadis

# Treatment with celastrol protects against obesity through suppression of galanin-induced fat intake and activation of PGC-1α/GLUT4 axis-mediated glucose consumption

Penghua Fang[a,c,1], Biao He[d,1], Mei Yu[a], Mingyi Shi[c], Yan Zhu[b], Zhenwen Zhang[b,*], Ping Bo[b,c]

[a] Department of Physiology, Nanjing University of Chinese Medicine Hanlin College, Taizhou, Jiangsu 225300, China
[b] Department of Endocrinology, Clinical Medical College, Yangzhou University, Yangzhou, Jiangsu 225001, China
[c] Jiangsu Key Laboratory of Integrated Traditional Chinese and Western Medicine for Prevention and Treatment of Senile Diseases, Medical College, Yangzhou University, Yangzhou 225001, China
[d] College of Physical Education, Anhui Normal University, Wuhu, Anhui 241003, China

ARTICLE INFO

*Keywords:*
Celastrol
Galanin
Obesity

ABSTRACT

Overweight and obesity may cause several metabolic complications, including type 2 diabetes mellitus and hyperlipidemia. Despite years of progress in medicine, there are no highly effective pharmacological treatments for obesity. The natural compound celastrol, a pentacyclic triterpene extracted from the roots of Tripterygium Wilfordi (thunder god vine) plant, exerts various bioactivities including anti-diabetic and anti-obese effects. Although celastrol could decrease food intake and obesity, the detailed mechanism for celastrol is still unclear as yet. Herein, we intended to determine the effect of celastrol on obesity and the underlying mechanisms. In the present study, diet-induced obese mice were treated with 100 μg/kg/d celastrol for the last 21 days, and 3T3-L1 cells were treated with celastrol for 6 h. The present findings showed that celastrol suppresses fat intake, and leads to weight loss by inhibiting galanin and its receptor expression in the hypothalamus of mice fed a high-fat diet. More importantly, in addition to these direct anti-obesity activities, celastrol augmented the PGC-1α and GLUT4 expression in adipocytes and skeletal muscles to increase glucose uptake through AKT and P38 MAPK activation. Celastrol also inhibited gluconeogenic activity through a CREB/PGC-1α pathway. In conclusion, the weight-lowering effects of celastrol are driven by decreased galanin-induced food consumption. Thus, this study contributes to our understanding of the anti-obese role of celastrol, and provides a possibility of using celastrol to treat obesity in clinic.

## 1. Introduction

The rapid increase in the prevalence of overweight and obesity is becoming an important health problem. Overweight and obesity may cause several metabolic complications, including type 2 diabetes mellitus, hyperlipidemia, high cholesterol, hypertension as well as coronary artery disease [1]. Prevention and treatment of obesity will benefit the treatment of these related diseases. Despite years of progress in medicine, there are no highly effective pharmacological treatments for obesity. Thus, great effort is needed to investigate the molecular mechanisms controlling obesity and to develop novel pharmacological strategies to treat obesity and its complications.

The natural compound celastrol, a pentacyclic triterpene extracted from the roots of Tripterygium Wilfordi plant (a traditional Chinese herb), exerts various bioactivities including anti-diabetic and anti-obese effects [2]. Recent studies from animal models of diabetes and obesity illustrate that celastrol could alleviate obesity and insulin resistance [2]. Celastrol has been reported to have anti-obesity effects via inhibition of adipogenesis and metabolic disorder to increase energy expenditure and expression of mitochondrial genes in mice fed with high fat diet [3]. Celastrol improves nonalcoholic fatty liver disease (NAFLD) by reducing lipid synthesis and elevating the anti-oxidative and anti-inflammatory status in mice fed with high fat diet [4]. In vitro, celastrol increased adipocyte differentiation and lipolysis by regulating peroxisome proliferator-activated receptor gamma 2 (PPARγ2) and CCAAT/enhancer-binding protein alpha (C/EBPα) signaling in 3T3-L1 adipocytes [5]. Besides, treatment with celastrol increases the expression of heat shock transcription factor 1 (HSF1) and peroxisome proliferator-

* Corresponding author: Department of Endocrinology, Clinical Medical College, Yangzhou University, Yangzhou 225001, China.
*E-mail address:* physiolpep@sina.cn (Z. Zhang).
[1] Co-first author.

https://doi.org/10.1016/j.bbadis.2019.02.002
Received 9 August 2018; Received in revised form 14 January 2019; Accepted 4 February 2019
Available online 10 February 2019
0925-4439/ 

activated receptor-γ coactivator-1α (PGC-1α) in skeletal muscle and adipocytes of diet-induced obese mice [3], which can promote thermogenesis and the remodeling of white adipose tissues. Moreover, the previous work verified that celastrol treatment reduced body weight gain and food intake in both high fat-fed obese in diabetes (db/db) and leptin-deficient (ob/ob) mice by inhibiting ER stress and increasing STAT3-dependent leptin signaling [6]. Nevertheless, the detailed molecular basis of celastrol on food intake and obesity has not been sufficiently explored. Therefore, in this study we used diet-induced obese mice to determine the effect of celastrol on food intake and obesity and the underlying mechanisms.

## 2. Methods and procedures

### 2.1. Drugs and reagents

BCA™ protein assay kit from Pierce Chemical Company, Rockford, USA. Trizol reagent from Gibco Invitrogen Inc., Invitrogen, USA. Celastrol and 2-[N-(7-nitrobenz-2-oxa-1, 3-diazol-4-yl) amino]-2-deoxy-D-glucose (2-NBDG) were purchased from Sigma-Aldrich, USA. Antibodies against galanin (GAL) and galanin receptor 1 (GALR1) were acquired from Abcam, UK and Sigma-Aldrich, USA respectively. Antibodies against glucose transporter 4 (GLUT4) and PGC-1α were purchased from Merck Millipore Inc., Germany. Antibodies against glyceraldehyde-phosphate dehydrogenase (GAPDH) was purchased from BOSTER Inc., China. Antibodies against AKT, p-AKT, UCP1, CREB, p-CREB, ATF2, p-ATF2, p38 MAPK and p-p38 MAPK were acquired from Cell Signaling Technology Inc., USA. Antibodies against tubulin, SIRT1, G6Pase and PEPCK were acquired from Proteinteck Inc., China.

### 2.2. Animals

Six-week-old male C57BL/6J mice were kept in a standard laboratory condition of temperature 21 ± 2 °C, relative humidity 50 ± 15%, 12 h light-dark cycles, with water and food available ad libitum. All animals used were closely monitored to ensure that none lived through stress and discomfort. The mice were fed a high fat diet (20% carbohydrates, 21% protein and 59% fat) for 16 weeks. Then the obese mice were divided into two groups: obese control group ($n = 8$) and obese group with celastrol ($n = 8$). Besides, a normal diet (60% carbohydrates, 21% protein and 19% fat) group ($n = 8$) was set up. The mice in the obese group with celastrol were injected with 100 μg/kg celastrol intraperitoneally (i.p.) at 6:00 am every day for 21 days, while mice in the both control groups were treated with dimethyl sulfoxide (DMSO). During the 3 weeks treatment period, the body weight of mice was recorded every day. The food intake of all mice was measured once a week. All mice were fasted for 12 h and used for glucose tolerance test and insulin tolerance test as described below. All animals received human care and all study protocols were approved by the Animal Studies Committee of Yangzhou University.

### 2.3. Glucose tolerance and insulin tolerance tests

At the day before the insulin tolerance test, 1.5 g/kg glucose dissolved in sterile water was i.p. injected into the mice after an overnight fast (12 h). The blood glucose levels in the tail vein blood were monitored at 0, 15, 30, 60, 90 and 120 min after the glucose challenge using a Glucometer (HMD Biomedical, Taiwan). After fasted for 12 h, all animals were subcutaneously injected with insulin (1 U/kg). The glucose levels in the tail vein blood were quantified at 0, 15, 30 and 60 min after the insulin challenge using a Glucometer (HMD Biomedical, Taiwan). Fasting insulin assay was performed by ELISA under manufacturer instructions (USCN Life Science, Inc.). The assay range for insulin was 123.5–10,000 pg/ml, and intra-assay precision CV% < 10% and inter-assay precision CV% < 12%. The homeostasis model of insulin resistance (HOMA-IR) was calculated by fasting serum insulin concentration (mU/ml) × fasting blood glucose level (mmol/l)/22.5. All measurements were performed in duplicate and the mean of two measurements was considered.

### 2.4. Collection of blood sample and tissues

After fasted for 12 h all animals were sacrificed on the second day after the insulin tolerance test. Then 1 ml blood and epididymal adipose tissue, hypothalamus, liver as well as skeletal muscle were fast collected. In brief, the blood samples were collected in prechilled EDTA tubes containing 100 μl protease and phosphatase inhibitors (1 μg/ml) and were immediately centrifuged for 10 min at 3500 r.p.m., 4 °C within 30 min of collection. Plasma was separated into vials and stored at −80 °C until measurement. The tissues were rinsed, weighed and frozen at −80 °C for further analysis.

### 2.5. GAL and GALP assay

Fasting plasma GAL (Catalog: CSB-EL009191MO, CUSABIO, Inc. China) and GALP (Catalog: CSB-EL009222MO, CUSABIO, Inc. China) assays were performed by ELISA under manufacturer instructions. In brief, the 100 μl sample in each assay point was analyzed for the GAL or GALP content using an enzyme-linked immunosorbent assay. According to the manufacturer's specification, the assay range for GAL was 31.25 pg/ml–2000 pg/ml, and intra-assay precision CV% < 8% and inter-assay precision CV% < 10%. The assay range for GALP was 23.5 pg/ml–1500 pg/ml, and intra-assay precision CV% < 8% and inter-assay precision CV% < 10%. All measurements were performed in duplicate and the mean of two measurements was considered.

### 2.6. Cell culture

3T3-L1 cells (purchased from the cell bank of the Institute of Biochemistry and Cell Biology, Shanghai) were grown in DMEM supplemented with 10% FBS, 100 U/ml penicillin, 100 mg/ml streptomycin at 37 °C in an humidified atmosphere included 5% $CO_2$. The cells were plated at $2 \times 10^5$/well in 6-well plates and used at confluence after 24 h preincubation. At 1 day post-confluence (designated “day 0”), cell differentiation was induced with a mixture of methylisobutylxanthine (0.5 mM), dexamethasone (0.25 M), and insulin (10 μg/ml) in DMEM containing 10% NCS. On day 2 and thereafter, DMEM containing 10% FBS and insulin (10 μg/ml) only was subsequently replaced every 2 days. Differentiation was confirmed by visualization of lipid droplet formation. Lipid droplets within the differentiated adipocytes from 3T3-L1 cells were observed using a modified Oil Red O staining method after 10 days of adipogenic differentiation. Briefly, the cells were washed twice with PBS, and then fixed for 5 min with 4% formaldehyde. Fixed cells were incubated with Oil Red O for 30 min at room temperature, followed by three washes with PBS. Oil Red O was prepared by diluting 60 ml of stock solution (0.5 g in 100 ml of isopropanol) in 40 ml of distilled water and filtered through coarse filter paper prior to use. After staining with the Oil Red O, the cells were washed and photographed. After inducing differentiation of adipocytes, these differentiated cells were starved for 4 h, then treated with 0.25, 0.5, 1.0 μM celastrol for 6 h. The control was given vehicle (0.1%DMSO in DMEM).

### 2.7. 2-NBDG uptake in flow cytometry

The experiments were performed in 6 culture plates of 3T3-L1 adipocytes by treatment with 0.25, 0.5, 1 μM celastrol respectively. Then all culture medium was replaced with 1000 μl of culture medium in the absence or presence of 100 μM fluorescent 2-NBDG, incubated at 37 °C with 5% $CO_2$ for 30 min before flow cytometry analysis. The 2-NBDG uptake was stopped by removing the incubation medium and

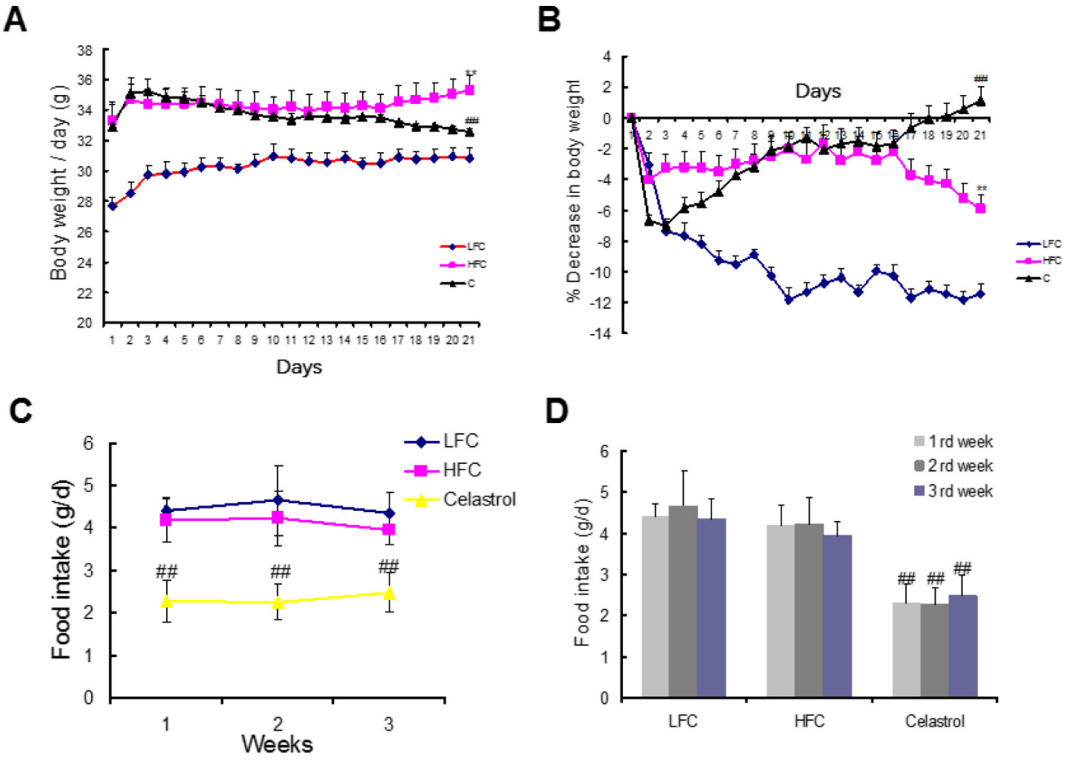


**Fig. 1.** The administration of celastrol for 21 days decreased the body weight and food intake in high fat diet-induced obese mice ($n$ = 8). (A) During the 3 weeks treatment period, the body weight of mice was measured. (B) The percent decrease (%) in body weight was measured after administration of celastrol for 21 days. (C) During the 3 weeks treatment period, the food intake of mice was measured. (D) The respective histograms of food intake were measured during the 3 weeks treatment period. LFC, low-fat diet control group; HFC, high-fat diet control group; Celastrol, high-fat diet group with celastrol. All data shown are the means ± SEM. $^{**}p < 0.01$ vs. LFC; $\#\#p < 0.01$ vs. HFC.

washing twice with cold phosphate buffered saline (PBS). The cells were subsequently resuspended in 300 µl pre-cold PBS for later flow cytometry analysis within 30 min at 4 °C. For each flow cytometric measurement, data from 15,000 single cell events were collected using a BD FACS calibur (Beckman Coulter FC500) flow cytometer within 20 s to analyze 2-NBDG fluorescence intensity.

### 2.8. Total RNA extraction and real-time PCR

Total RNA was extracted with Trizol from 100 mg frozen adipose tissues and hypothalamus. cDNA was synthesized from 1 µg RNA using MMLV reverse transcriptase. Real-time quantitative PCR was performed for gene expression levels using real-time fluorescent detection in an Applied Biosystems 7500 real-time PCR instrument (ABI 7500, USA). The oligonucleotide primers were as follows: GLUT4 Forward Sequence 5′-GGCTTTGTGGCCTTCTTTGAG-3′, Reverse Sequence5′-GACCCATAG CATCCGCAACAT-3′; PGC-1α Forward Sequence5′-ACCATGACTACTG TCAGTCACTC-3′, Reverse Sequence5′-GTCACAGGAGGCATCTTTG AAG-3′; GAL Forward Sequence 5′-GAGCCTTGATCCTGCACTGA -3′, Reverse Sequence 5′-AGTGGCTGACAGGGGTCACAA -3′; GALR1 Forward Sequence 5′-CCAAGGGGGTATCCCAGTAA -3′, Reverse Sequence 5′-GGCCAAACACTACCAGCGTA -3′; GALR2 Forward Sequence 5′-ATAGTGGTGGCATGCTGGAA -3′, Reverse Sequence 5′-AGGCTGGATCGAGGGTTCTA -3′; GALR3 Forward Sequence 5′-ATC TTCCTGTTGGGCATGGT-3′, Reverse Sequence 5′-TGTACCGTCTTGCA CACGAA-3′; Leptin Forward Sequence 5′-CTCCAAGGTTGTCCAGG GTT-3′, Reverse Sequence 5′-AAAACTCCCCACAGAATGGG-3′; NPY Forward Sequence 5′-AATCAGTGTCTCAGGGCTG -3′, Reverse Sequence 5′-CTATCTCTGCTCGTGTGTTT-3′; GAPDH Forward Sequence 5′-AGAACATCATCCCTGCATCC-3′, Reverse Sequence 5′-TCCACCACCC TGTTGCTGTA-3′. Amplification condition was: an initial denaturation at 95 °C for 10 min; 95 °C for 15 s, 62 °C for 60 s, 40 cycles. The $2^{-\Delta\Delta CT}$ method was used to analyze the PCR data.

### 2.9. Western blot analysis

Total proteins of tissue or 3T3-L1 cell samples were extracted using RIPA agents and quantified with BCA protein assay kit to determine protein levels. Briefly, fifty micrograms of samples were separated by a 12% sodium dodecyl sulfate-polyacrylamide gel electrophoresis and transferred to a polyvinylidene difluoride filter membranes. Membranes were blocked in Tris-buffered saline (pH 7.5) containing 0.05% Tween-20 (1 × TBST) and 5% skimmed milk for 2 h, then probed overnight at 4 °C with an antibody against GAPDH, Tubulin, GLUT4, GAL, GALR1, PGC-1α, AKT, p-AKT, UCP1, ATF2, p-ATF2, CREB, p-CREB, SIRT1, PEPCK, G6pase, p38 MAPK and p-p38 MAPK respectively. Membranes were washed with 1 × TBST for 10 min and incubated for 2 h with horseradish peroxidase-conjugated secondary antibody. Lastly, immunoreactive bands were visualized by chemiluminescence and quantified by densitometry using a Quantity One Analysis Software (Bio-Rad).

### 2.10. Statistical analysis

SPSS 17.0 for Windows was used for statistical analysis. Comparisons between the means of three groups were analyzed by one-way ANOVA with Duncan's tests. Data were presented as mean ± SEM with $p < 0.05$ as the limit for statistical significance.

## 3. Results

### 3.1. The lowering effect of celastrol on fat intake and body weight of obese mice

All mice used in this experiment exhibited similar body weight and food intake at the beginning of the experiment. Upon feeding of a high-fat diet for 16 weeks, the mice started to demonstrate a significant increase in body weight compared with age- and gender-matched mice on a normal diet. At the end of three weeks treatment, the body weight was significantly increased in the obese control group compared with the normal controls ($p < 0.01$). However, the body weight was significantly decreased in treatment with celastrol group compared with the obese controls ($p < 0.01$) (Fig. 1A). Besides, the percent decrease (%) in body weight was significantly increased in treatment with celastrol group compared with the obese control group ($p < 0.01$) (Fig. 1B). As shown in Fig. 1C and D, the food intake of mice was significantly decreased in the celastrol group compared with the obese controls in the first, second and third week, respectively ($p < 0.01$). These results suggest that celastrol decreases food intake and body weight.

### 3.2. Effect of celastrol on hyperglycemia and insulin resistance in obese mice

As shown in Fig. 2A and B, the fasting insulin and glucose levels were significantly elevated in the obese control group compared with the normal controls ($p < 0.01$). During the glucose tolerance test, as shown in Fig. 2C, the circulating glucose levels were markedly increased in the fasted state and in response to glucose load in the obese control group compared with normal controls ($p < 0.01$). As shown in Fig. 2D, the circulating glucose levels were markedly increased in the fasted state and in response to insulin load in the obese control group compared with normal controls during the insulin tolerance test ($p < 0.01$). Besides, the HOMA-IR was significantly increased in the obese control mice compared with normal control mice ($p < 0.01$) (Fig. 2E).

However, celastrol-treated mice displayed a significant decrease in the severity of obesity-associated systemic insulin resistance and glucose intolerance compared with obese control mice (Fig. 2A–E). After 21 days of injection with celastrol, the mice had a decrease of fasting hyperglycemia ($p < 0.05$) (Fig. 2A) and an improvement in glucose and insulin tolerance associated with a decrease in plasma glucose levels in the fasted state and in response to glucose or insulin load ($p < 0.05$) (Fig. 2C–D). However, we did not observe significant variation of plasma insulin in response to celastrol treatment compared with obese control mice ($p > 0.05$) (Fig. 2B). This strongly suggests celastrol-induced reduction in glucose stems from effects on insulin sensitivity, rather than on insulin levels. Moreover, the HOMA-IR was significantly lower in celastrol-treated mice than in obese control mice (Fig. 2E) ($p < 0.05$). These results strongly suggest that celastrol improves systemic insulin sensitivity and glucose homeostasis.

### 3.3. Effect of celastrol on plasma GAL and GALP levels

As shown in Fig. 3A and B, the fasting GAL and GALP levels were significantly elevated in the obese control group compared with the normal controls ($p < 0.01$). However, after 21 days of injection with celastrol, the mice displayed a significant decrease in the plasma GAL and GALP compared with obese control mice ($p < 0.01$) (Fig. 3A–B). These results may suggest that celastrol inhibits food intake and decreases body weight by the reduction of GAL and GALP.

### 3.4. Celastrol treatment increases glucose uptake in adipocytes

As shown in Fig. 4, the 2-NBDG uptake in the celastrol group compared with the controls was significantly elevated after treatment with 0.25, 0.5, 1.0 μM celastrol respectively ($p < 0.01$). These results suggest that celastrol improves glucose uptake in the absence of insulin.

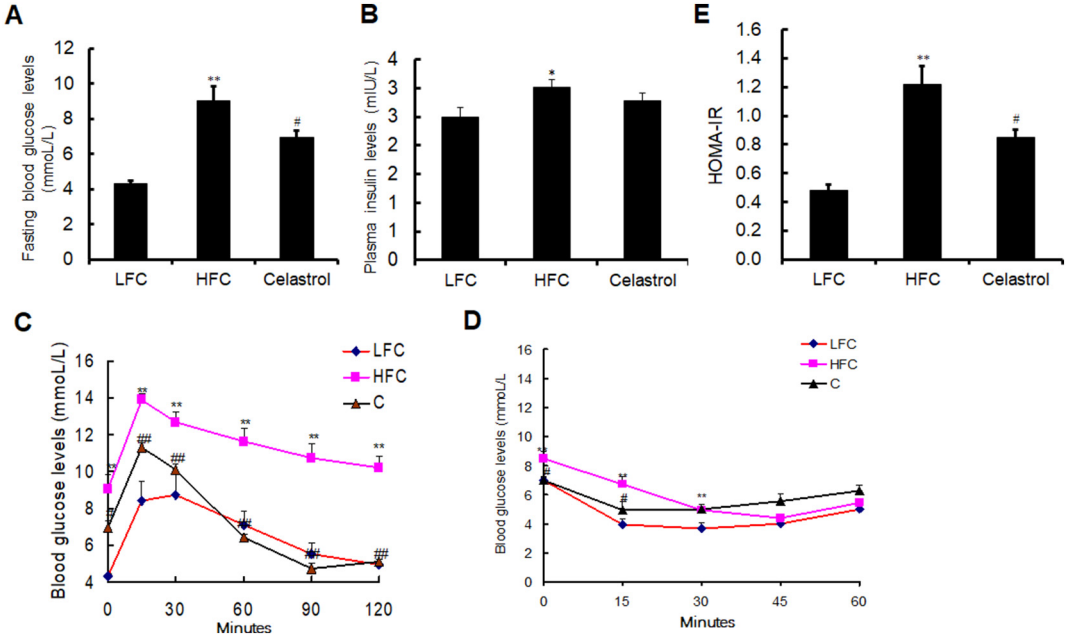


**Fig. 2.** Celastrol-treated mice displayed a significant decrease in the severity of obesity-associated systemic insulin resistance and glucose intolerance compared with obese control mice ($n = 6–8$). (A) Blood glucose levels were lower in the celastrol group than obese controls. (B) It is not observe significant variation of plasma insulin in response to this treatment compared with obese control mice. (C) Glucose tolerance tests (GTT). After 21 days of administration of celastrol, the mice have decreased fasting hyperglycemia and an improvement in glucose tolerance associated with a decrease in plasma glucose levels in the fasted state and in response to glucose load. (D) Insulin tolerance tests (ITT). After 21 days of administration of celastrol, the mice have an improvement in insulin tolerance associated with a decrease in plasma glucose levels in response to glucose load. (E) HOMA-IR index. HOMA-IR index in the celastrol group was significantly decreased compared with obese controls, but that increased in obese controls compared with normal controls. LFC, low-fat diet control group; HFC, high-fat diet control group; C, high-fat diet group with celastrol. All data shown are the means ± SEM. *$p < 0.05$ & **$p < 0.01$ vs. LFC; #$p < 0.05$ & ##$p < 0.01$ vs. HFC.

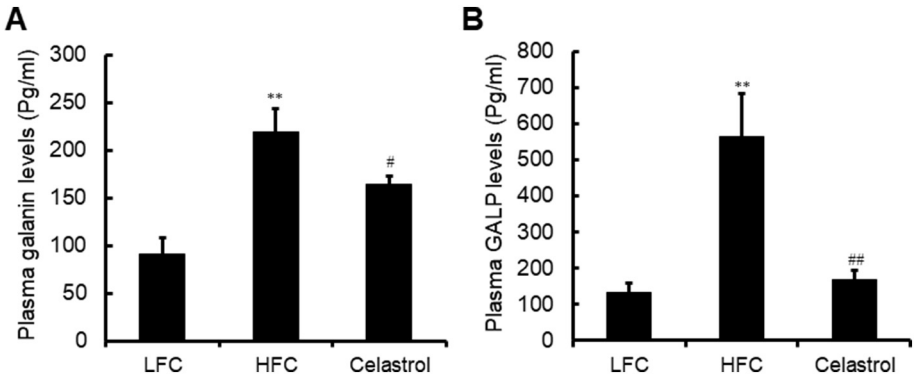


**Fig. 3.** Celastrol decreases plasma GAL and GALP levels in high fat diet-induced obese mice ($n = 8$). (A) Compared with obese control mice, celastrol-treated mice displayed a marked decrease in levels of plasma GAL. (B) Compared with obese control mice, celastrol-treated mice displayed a marked decrease in levels of plasma GALP. LFC, low-fat diet control group; HFC, high-fat diet control group; Celastrol, high-fat diet group with celastrol. All data shown are the means ± SEM. $^{**}p < 0.01$ vs. LFC; $\#p < 0.05$ & $\#\#p < 0.01$ vs. HFC.

### *3.5. Celastrol suppresses the expression of leptin, NPY, GAL and its receptors in the hypothalamus of obese mice*

As shown in Fig. 5A–F, the GAL mRNA, GALR1 mRNA, GALR2 mRNA, GALR3 mRNA, leptin mRNA and NPY mRNA expression levels were significantly increased in hypothalamus of obese control group compared with the normal controls ($p < 0.01$). Compared with obese control mice, celastrol-treated mice displayed a marked reduction in levels of GAL mRNA, GALR1 mRNA, GALR3 mRNA, leptin mRNA and NPY mRNA expression of hypothalamus ($p < 0.01$) (Fig. 5A–F). However, we did not observe significant variation of GALR2 mRNA in response to celastrol treatment compared with obese control mice ($p > 0.05$) (Fig. 5C). This suggests that celastrol-induced reduction in fat intake and weight loss stems from effects of leptin, NPY, GAL and GALR1/3.

As shown in Fig. 5G–I, the GAL and GALR1 contents in the hypothalamus of obese control mice were markedly increased compared with that in normal control mice ($p < 0.01$). Upon treatment with celastrol, the GAL and GALR1 contents in hypothalamus were markedly reduced compared with that in obese control mice ($p < 0.01$) (Fig. 5G–I). Taken together, these results suggest that celastrol inhibition of food intake involves in a decrease in GAL and GALR1/3 expression of hypothalamus.

### *3.6. Celastrol treatment increases PGC-1α and its target genes expression levels in adipocytes*

As shown in Fig. 6A–D, the mRNA and protein levels of GLUT4 and PGC-1α were significantly decreased in adipocytes of obese control group compared with the normal controls ($p < 0.01$). Compared with obese control mice, celastrol-treated mice displayed a marked increase in mRNA and protein levels of GLUT4 and PGC-1α of adipocytes ($p < 0.01$) (Fig. 6A–D). These results suggest that celastrol amelioration of insulin resistance involves in an increase in PGC-1α and GLUT4

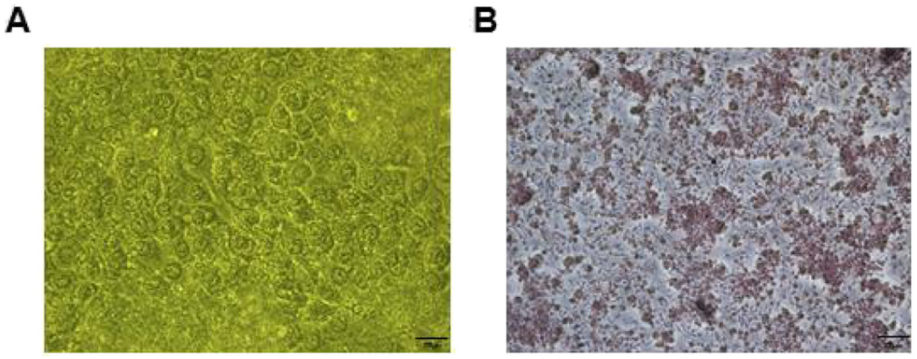


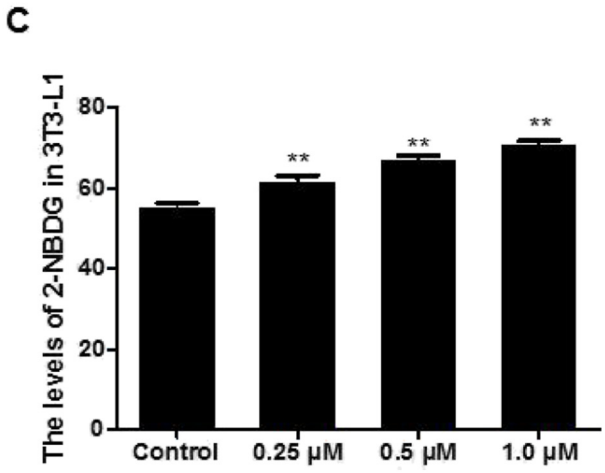


**Fig. 4.** The administration of celastrol significantly increased the fluorescence 2-NBDG intensity of 3T3-L1 adipocytes ($n = 3$). (A) Lipid droplets within the differentiated adipocytes from 3T3-L1 cells were observed and photographed after 10 days of adipogenic differentiation. (B) Following10 days of treatment after adipogenic differentiation, the cultures were stained with Oil red O, then visualized and photographed. (C) The 2-NBDG uptake of cells in the celastrol group compared with controls was significantly elevated after treatment with 0.25, 0.5, 1.0 μM celastrol respectively. All data shown are the means ± SEM. $^{**}p < 0.01$ vs. controls.

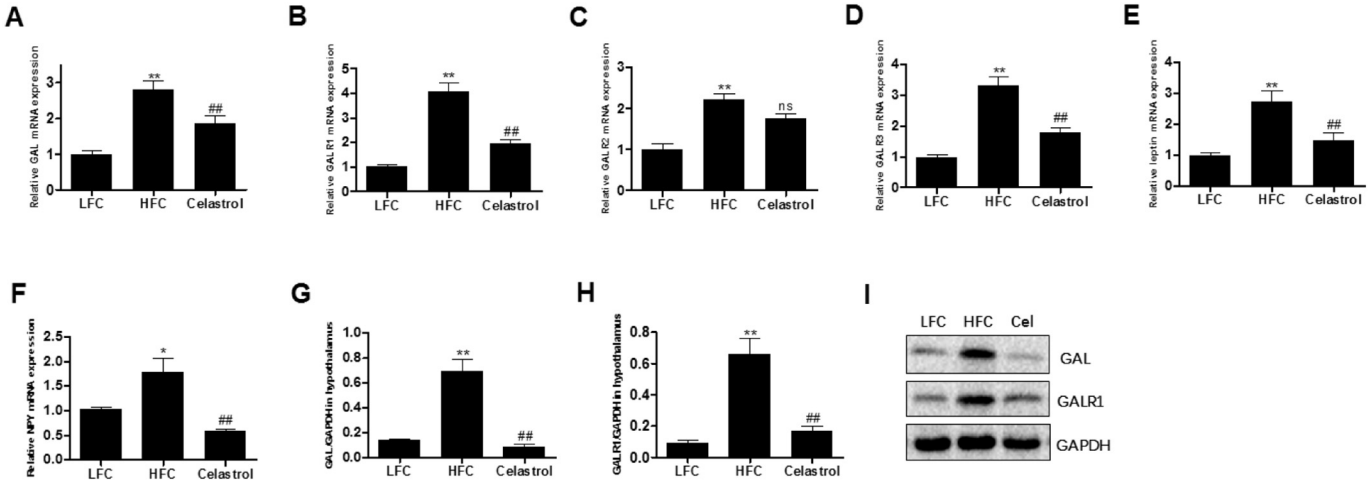


**Fig. 5.** Celastrol suppresses the expression of leptin, NPY, GAL and its receptors in the hypothalamus of obese mice ($n$ = 3–5). (A) GAL mRNA expression of hypothalamus. Compared with obese control mice, celastrol-treated mice displayed a marked decrease in levels of GAL mRNA expression of hypothalamus. (B) GALR1 mRNA expression of hypothalamus. Compared with obese control mice, celastrol-treated mice displayed a marked decrease in levels of GALR1 mRNA expression of hypothalamus. (C) GALR2 mRNA expression of hypothalamus. Compared with obese control mice, celastrol-treated mice displayed a slight reduction in levels of GALR2 mRNA expression of hypothalamus. (D) GALR3 mRNA expression of hypothalamus. Compared with obese control mice, celastrol-treated mice displayed a marked decrease in levels of GALR3 mRNA expression of hypothalamus. (E) Leptin mRNA expression of hypothalamus. Compared with obese control mice, celastrol-treated mice displayed a marked decrease in levels of leptin mRNA expression of hypothalamus. (F) NPY mRNA expression of hypothalamus. Compared with obese control mice, celastrol-treated mice displayed a marked decrease in levels of NPY mRNA expression of hypothalamus. (G) The GAL contents in the hypothalamus. Upon treatment with celastrol, the GAL contents in the hypothalamus were markedly decreased compared with that in obese control mice. (H) The GALR1 contents in the hypothalamus. Upon treatment with celastrol, the GALR1 contents in the hypothalamus were markedly decreased compared with that in obese control mice. (I) The representative Western blot lines of GAL and GALR1 in the hypothalamus. GAPDH was used as the loading control. LFC, low-fat diet control group; HFC, high-fat diet control group; Celastrol, high-fat diet group with celastrol. All data shown are the means ± SEM. $*p < 0.05$ & $**p < 0.01$ vs. LFC; $\#p < 0.05$ & $\#\#p < 0.01$ vs. HFC. ns, not significant.

expression of adipocytes.

To further determine the molecular mechanism of PGC-1α regulation by celastrol, we have examined the activation status of AKT, UCP1 and ERK by immunoblotting with antibodies recognizing active phosphorylated forms of these proteins in adipocytes. As shown in Fig. 6E–H, the phosphorylated AKT and UCP1 in adipocytes of obese control mice were markedly decreased compared with that in normal control mice ($p < 0.01$), while the phosphorylated ERK in adipocytes of obese control mice was markedly increased compared with that in normal control mice ($p < 0.01$). Western blot analysis indicated that UCP1 and phosphorylation of AKT in adipocytes were markedly enhanced by celastrol treatment ($p < 0.01$), while phosphorylation of ERK was markedly reduced by celastrol treatment ($p < 0.01$) (Fig. 6E–H). In vitro, after treatment with 0.25, 0.5, 1.0 μM celastrol in 3T3-L1 cells, the levels of PGC-1α and GLUT4 were significantly enhanced compared with control (Fig. 6I–J). Besides, the levels of the phosphorylated AKT and UCP1 protein were significantly increased in celastrol-treated 3T3-L1 cells compared with control, while the level of phosphorylated ERK was significantly decreased compared with control (Fig. 6K–N). Taken together, these results suggest that celastrol elevates PGC-1α, UCP1 and GLUT4 protein levels in adipose tissues to alleviate insulin resistance dependent of AKT and ERK phosphorylation.

### 3.7. Celastrol treatment increases PGC-1α and its target genes expression levels of skeletal muscle of obese mice

As shown in Fig. 7A–D, the protein levels of GLUT4 and PGC-1α were significantly decreased in skeletal muscles of obese control group compared with the normal controls ($p < 0.01$). Compared with obese control mice, celastrol-treated mice displayed a marked increase in levels of GLUT4 and PGC-1α expression of skeletal muscles ($p < 0.01$) (Fig. 7A–D). These results suggest that celastrol amelioration of insulin resistance involves in an increase in PGC-1α and GLUT4 expression of skeletal muscles.

To further determine the molecular mechanism of PGC-1α regulation by celastrol, we have examined the activation status of ATF2 and p38MAPK by immunoblotting with antibodies recognizing active phosphorylated forms of these proteins in skeletal muscles. As shown in Fig. 7E–G, the levels of phosphorylated ATF2 and p38MAPK in skeletal muscles of obese control mice were markedly diminished compared with that in normal control mice ($p < 0.01$). Upon treatment with celastrol, the levels of phosphorylated ATF2 and p38MAPK in skeletal muscles were markedly increased compared with that in obese control mice ($p < 0.01$) (Fig. 7E–G). These data predicted that celastrol may regulate PGC-1α expression of skeletal muscles through a p38 MAPK/ATF2 pathway.

### 3.8. Celastrol inhibits hepatic gluconeogenesis via the regulation of CREB/PGC-1α signaling pathway

The dysregulation of gluconeogenesis is responsible for fasting hyperglycemia in diabetes. The hepatic gluconeogenesis is under the control of two key rate limiting enzymes: G6Pase and PEPCK. Therefore, we analyzed the levels of G6pase and PEPCK in liver. We found that levels of both G6pase and PEPCK expression were significantly increased in liver of obese control mice compared with those in normal control mice ($p < 0.01$), while celastrol treatment significantly inhibited the levels of G6pase and PEPCK expression of liver in mice compared with those in obese control mice ($p < 0.05$) (Fig. 8A and B). These results suggesting that celastrol reduces G6Pase and PEPCK levels to inhibit gluconeogenic activity, resulting in the decrease in hepatic glucose production.

We further explored the mechanism of celastrol regulation of gluconeogenic activity by assessing the expression of the signal transducer and activator of PGC-1α, SIRT1 and CREB in liver. Here, we found that the protein expression levels of PGC-1α, SIRT1 and p-CREB of liver were significantly higher in obese control mice than in the normal control mice ($p < 0.01$) (Fig. 8C–F). Celastrol treatment significantly decreased the expression levels of PGC-1α and p-CREB in liver of mice compared with the obese control mice ($p < 0.01$), while the level of

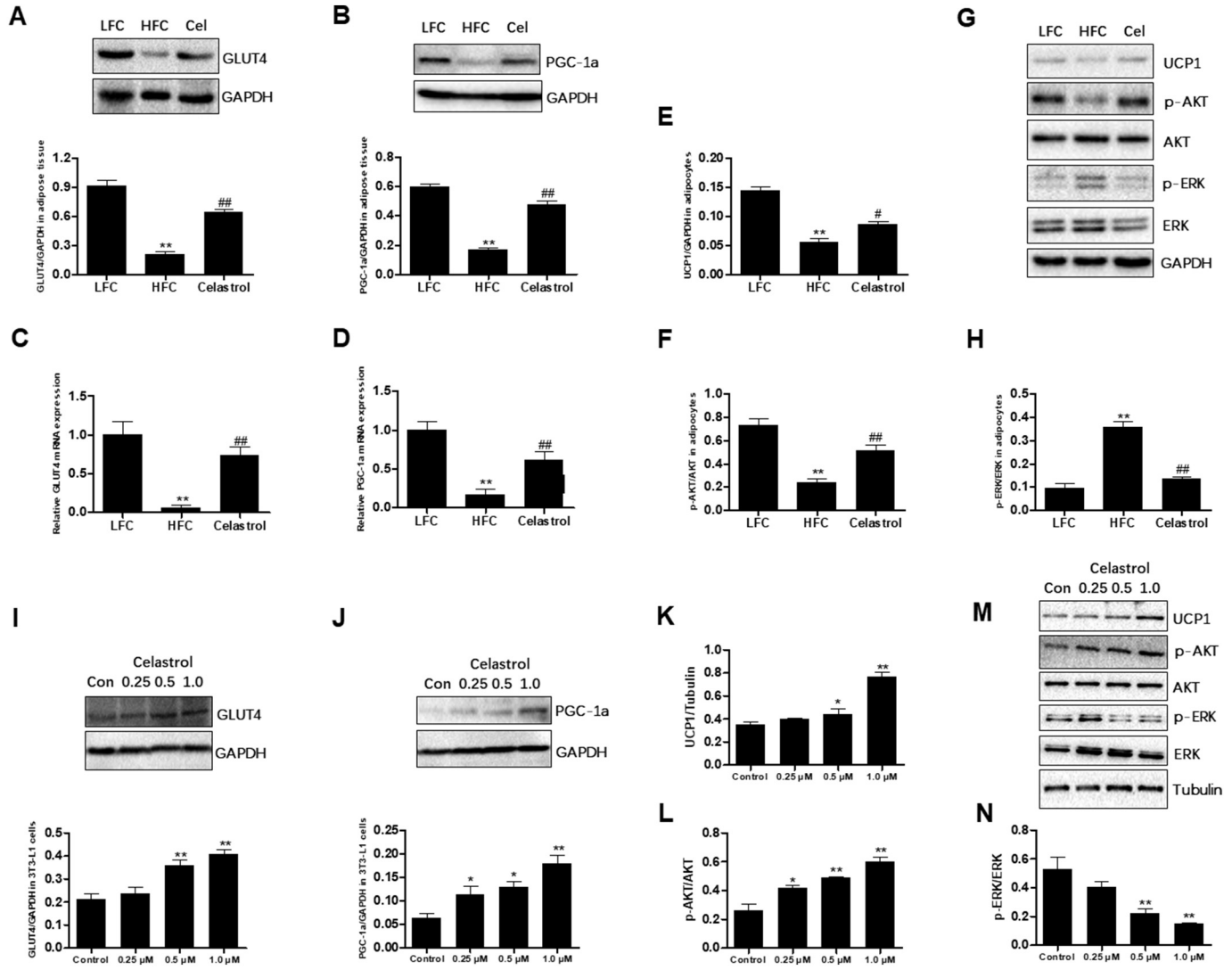


**Fig. 6.** Celastrol treatment increases PGC-1α and its target genes expression levels in adipocytes ($n = 8$). (A) GLUT4 protein of adipocytes. Compared with obese control mice, celastrol-treated mice displayed a marked increase in levels of GLUT4 protein expression of adipocytes. (B) PGC-1α protein of adipocytes. Compared with obese control mice, celastrol-treated mice displayed a marked increase in levels of PGC-1α protein of adipocytes. (C) GLUT4 mRNA expression of adipocytes. Compared with obese control mice, celastrol-treated mice displayed a marked increase in levels of GLUT4 mRNA expression of adipocytes. (D) PGC-1α mRNA expression of adipocytes. Compared with obese control mice, celastrol-treated mice displayed a marked increase in levels of PGC-1α mRNA expression of adipocytes. (E) UCP1 protein of adipocytes. Compared with obese control mice, celastrol-treated mice displayed a marked increase in levels of UCP1 protein expression of adipocytes. (F) The ratio of p-AKT/AKT of adipocytes. Compared with obese control mice, celastrol-treated mice displayed a marked increase in levels of phosphorylated AKT of adipocytes. (G) The representative Western blot lines of UCP1, p-AKT, AKT, p-ERK and ERK in adipocytes. GAPDH was used as the loading control. (H) The ratio of p-ERK/ERK of adipocytes. Compared with obese control mice, celastrol-treated mice displayed a marked decrease in levels of phosphorylated ERK of adipocytes. (I) GLUT4 contents in 3T3-L1 adipocytes. Upon treatment with celastrol, the levels of GLUT4 in adipocytes were markedly increased compared with that in control group. (J) PGC-1α contents in 3T3-L1 adipocytes. Upon treatment with celastrol, the levels of PGC-1α in adipocytes were markedly increased compared with that in control group. (K) UCP1 protein in 3T3-L1 adipocytes. Upon treatment with celastrol, the levels of UCP1 in adipocytes were markedly increased compared with that in control group. (L) The ratio of p-AKT/AKT in 3T3-L1 adipocytes. Upon treatment with celastrol, the levels of p-AKT in adipocytes were markedly increased compared with that in control group. (M) The representative Western blot lines of UCP1, p-AKT, AKT, p-ERK and ERK in 3T3-L1 adipocytes. Tubulin was used as the loading control. (N) The ratio of p-ERK/ERK in 3T3-L1 adipocytes. Upon treatment with celastrol, the levels of p-ERK in adipocytes were markedly increased compared with that in control group. LFC, low-fat diet control group; HFC, high-fat diet control group; Celastrol, high-fat diet group with celastrol. All data shown are the means ± SEM. $*p < 0.05$ & $**p < 0.01$ vs. control or LFC; $\#p < 0.05$ & $\#\#p < 0.01$ vs. HFC.

SIRT1was slightly changed in liver of celastrol-treated mice (Fig. 8C–F). These data predicted that celastrol may regulate gluconeogenic activity through a CREB/PGC-1α pathway.

## 4. Discussion

Previous studies have shown that celastrol treatment significantly decreased body weight due to decreases in food consumption [6]. Consistent with these findings, we found that the body weight and food intake were significantly decreased in treatment with celastrol mice compared with the obese control mice. These results suggest that celastrol decreases food intake and body weight. Although it is not clear why the celastrol group showed lower body weight and decreased food intake, our results suggest that inhibition of food intake with celastrol may decrease levels of GAL and GALR1/3 in the hypothalamus. GAL, a 29/30-amino-acid neuropeptide, is undoubtedly involved in the regulation of food intake and body weight [7]. First, fed with a high-fat diet, rats showed an increase in GAL level and proliferation of GAL-

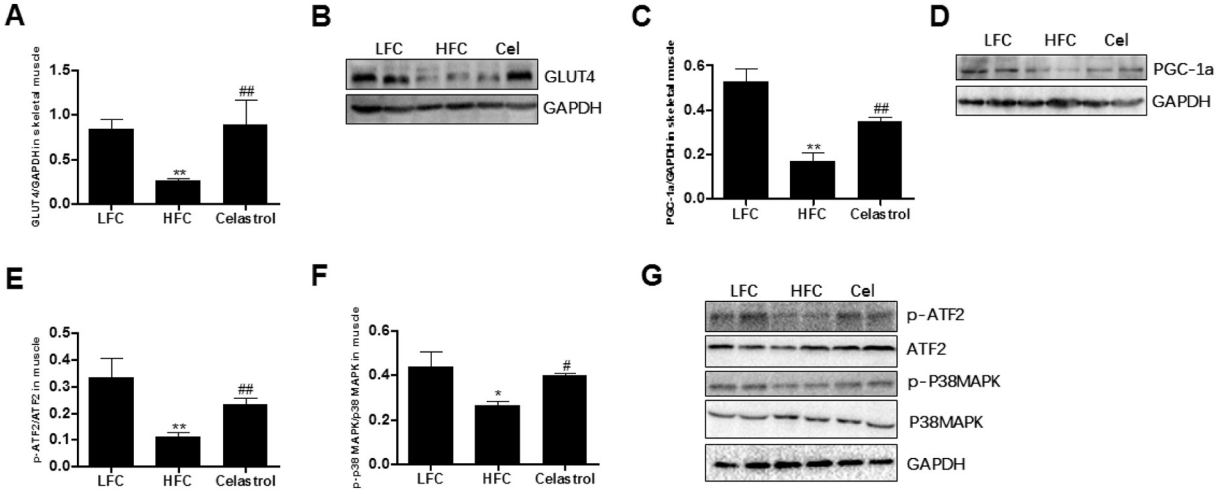


**Fig. 7.** Celastrol treatment increases PGC-1α and its target genes expression levels of skeletal muscle of obese mice ($n$ = 8). (A) GLUT4 protein of skeletal muscle. Compared with obese control mice, celastrol-treated mice displayed a marked increase in levels of GLUT4 protein expression of skeletal muscle. (B) The representative Western blot lines of GLUT4 in skeletal muscle. GAPDH was used as the loading control. (C) PGC-1α protein of skeletal muscle. Compared with obese control mice, celastrol-treated mice displayed a marked increase in levels of PGC-1α protein of skeletal muscle. (D) The representative Western blot lines of PGC-1α in skeletal muscle. GAPDH was used as the loading control. (E) The ratio of p-ATF2/ATF2 of skeletal muscle. Compared with obese control mice, celastrol-treated mice displayed a marked increase in levels of phosphorylated ATF2 of skeletal muscle. (F) The ratio of p-P38MAPK/ P38MAPK of skeletal muscle. Compared with obese control mice, celastrol-treated mice displayed a marked increase in levels of phosphorylated P38MAPK of skeletal muscle. (G) The representative Western blot lines of p-ATF2, ATF2, p-P38MAPK and P38MAPK in skeletal muscle. GAPDH was used as the loading control. LFC, low-fat diet control group; HFC, high-fat diet control group; Celastrol, high-fat diet group with celastrol. All data shown are the means ± SEM. $*p < 0.05$ & $**p < 0.01$ vs. LFC; $\#p < 0.05$ & $\#\#p < 0.01$ vs. HFC.

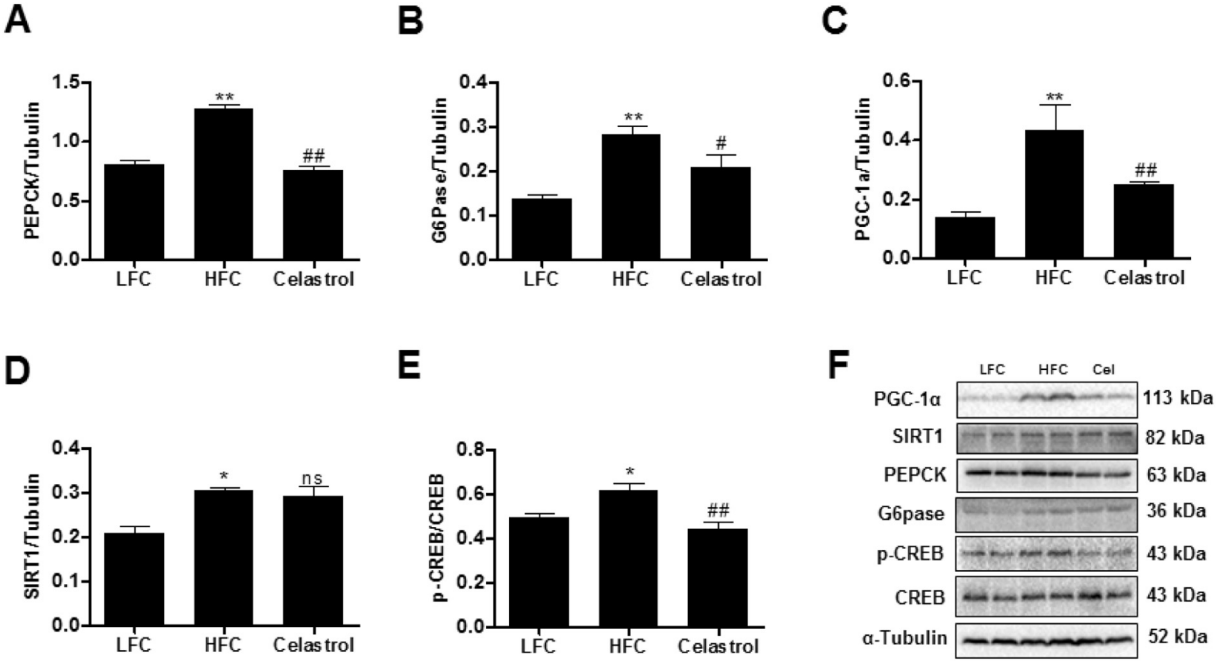


**Fig. 8.** Celastrol inhibits hepatic gluconeogenesis via the regulation of CREB/PGC-1α signaling pathway ($n$ = 8). (A) PEPCK protein of liver. Compared with obese control mice, celastrol-treated mice displayed a marked decrease in levels of PEPCK protein expression of liver. (B) G6pase protein of liver. Compared with obese control mice, celastrol-treated mice displayed a marked decrease in levels of G6pase protein expression of liver. (C) PGC-1α protein of liver. Compared with obese control mice, celastrol-treated mice displayed a marked decrease in levels of PGC-1α protein expression of liver. (D) SIRT1 protein of liver. Compared with obese control mice, celastrol-treated mice displayed a slight change in levels of SIRT1 protein expression of liver. (E) The ratio of p-CREB/CREB of liver. Compared with obese control mice, celastrol-treated mice displayed a marked decrease in levels of phosphorylated CREB of liver. (F) The representative Western blot lines of PEPCK, G6pase, PGC-1α, SIRT1, p-CREB and CREB in liver. Tubulin was used as the loading control. LFC, low-fat diet control group; HFC, high-fat diet control group; Celastrol, high-fat diet group with celastrol. All data shown are the means ± SEM. $*p < 0.05$ & $**p < 0.01$ vs. LFC; $\#p < 0.05$ & $\#\#p < 0.01$ vs. HFC. ns, not significant.

producing neurons in the hypothalamus [8,9]. In contrast, a stimulatory effect of GAL, intracerebroventricular (i.c.v.) injected directly into paraventricular nucleus (PVN), significantly enhanced daily caloric intake and weight of fat depots [10]. Besides, heterozygous GAL over-expressive mice increased the intake of a fat-rich diet by 55% than wild-type mice [11], while GAL knockout mice decreased the intake of fat-rich diet by 48% than controls [12]. Furthermore, chronic administration of GAL by mini-osmotic pumps into the lateral ventricle of GAL knockout mice partially reversed the fat avoidance phenotype [13]. More interestingly, a wealth of evidence revealed that central GAL-induced increase in food intake and body weight is mainly mediated by GALR1 [7]. These suggest that GAL-GALR1 systems help adapt food intake and metabolism to changes in dietary fat. Of note, celastrol has been reported to cross the brain-blood barrier [14]. Results in this study illustrated that the increased abundance of GAL, GALR1 and GALR3 in the hypothalamus of obese mice were highly down-regulated by celastrol treatment, which might indicate that celastrol could reduce fat intake by inhibition of the GAL-GALR1/3 system and subsequently promote the weight loss in obese mice. Moreover, galanin may interact with other appetite-regulating peptides, such as leptin and NPY, to control the appetite and obesity levels of animals [7]. The low GAL and GAL1 mRNA expression in the LHA of GAL-LepRb KO mice consume less high fat diet [15]. The celastrol-treated mice also displayed a marked reduction in levels of leptin and NPY expression of hypothalamus in this study. Our data corroborate previously reported that celastrol strongly decreases the levels of leptin and NPY expression in the hypothalamus of obese mice [6]. Therefore, low GAL and GAL1/3 expression in the hypothalamus of celastrol-treated mice could sufficiently explain the observed decrease in fat consumption. The present study provides evidence that celastrol suppresses food intake, and leads to weight loss by inhibiting GAL and GALR1/3 expression in the hypothalamus of mice fed a high-fat diet.

Additionally, celastrol has been shown to inhibit galanin-like peptide (GALP). GALP was discovered in 1999 in the porcine hypothalamus [16]. GALP is a 60 amino-acid neuropeptide that shares sequence homology with galanin (1 − 13) in position 9–21 and can bind to and activate the three galanin subtype receptors (GALR1–3) [16]. Considerable evidence now supports that GALP stimulates feeding behavior and body weight as well as influences energy metabolism and homeostasis [7]. Also, we have previously demonstrated that obese individuals have higher plasma GAL and GALP concentrations and both peptide concentrations were positively correlative to TG concentrations in obese human [17]. In agreement with these results, the fasting GAL and GALP levels were significantly elevated in the obese control group compared with the normal controls. It is possible that high fat diet induced secretion of galanin is originated both from nerve endings and soma/dendrites of the central nervous system or peripheral tissues, such as gastrointestinal tract, adipose tissue and sympathetic nerve endings. It is plausible that, in diet-induced obesity, the elevated blood level of GAL and GALP will upregulate the expression of the GALR1 located in the hypothalamus, which may, in turn, stimulate the GAL-mediated signaling pathways in the hypothalamus. We found that celastrol possesses an effect on reducing levels of blood GAL and GALP. These results further indicate that celastrol exerts anti-obese effect by suppressing food intake and body weight via the inhibition of GAL system.

Celastrol was reported to induce antihyperglycemic effects and ameliorate insulin resistance [3]. The antihyperglycemic activity of celastrol was observed in mice fed a high-fat diet [18]. In vitro, celastrol increased glucose uptake and consumption in C2C12 myotubes [19]. Consistent with several lines of studies, our date demonstrated that celastrol treatment reversed high fat diet-induced glucose intolerance, hyperglycemia and insulin resistance in diet-induced obese mice. Besides, celastrol was found to improve glucose uptake of 3T3-L1 cells. Therefore, all of these results provide evidence in support of a role for celastrol in increasing glucose uptake and insulin sensitivity.

About 90% of insulin-stimulated glucose uptake occurs both in skeletal muscle and adipose tissue [20]. Thus, understanding glucose transport mechanism in both skeletal muscles and adipocytes is crucial for elucidating the mechanisms that underlie the effect of celastrol on glucose metabolism. Celastrol appears to induce the expression of many genes associated with the function of glucose transport and metabolism in skeletal muscles and adipocytes [3]. The levels of PGC-1α, UCP1 and GLUT4 are major indexes that reflect the activity of glucose uptake and energy expenditure in fat and muscle tissues [20,21]. Besides, PGC-1α can enhance the expression of GLUT4 and UCP1 to increase glucose uptake and metabolism [22–24]. Results in this study illustrated that the decreased abundance of PGC-1α, UCP1 and GLUT4 in fat and muscle tissues of obese mice were highly up-regulated by celastrol treatment, which might indicate that celastrol could promote the uptake and utilization of glucose by activating the PGC-1α/GLTU4 or PGC-1α/UCP1 pathway and subsequently reduce the blood glucose level in diabetic mice. Taken together, our data suggest that pharmacological activation of the PGC1a/GLUT4 axis with celastrol enhances glucose metabolism.

Activated AKT of adipocytes may prevent insulin resistance, while phosphorylation of ERK may cause insulin resistance of adipocytes [25,26]. Our results showed that treatment with celastrol enhanced the phosphorylated AKT contents, and inhibited the phosphorylation of ERK in adipocytes, suggesting that celastrol potently increased insulin sensitivity, and inhibited proinflammatory responses in the adipocytes. To further confirm the animal experiment results, we used 3T3-L1 adipocytes in a cell culture model. As expected, the phosphorylation of ERK level was decreased after treatment celastrol in 3T3-L1 adipocytes, while the phosphorylation of AKT level was increased. Collectively, celastrol exerted an effect on high fat diet-induced insulin resistance in adipocytes via regulation of AKT and ERK signaling pathways.

Depending on tissue types, PGC-1α expression is regulated differentially by distinctive signaling pathways and transcription regulators. For example, ATF2 and p38 MAPK play critical roles in the regulation of PGC-1α expression in skeletal muscles [27]. P38 MAPK is a key regulator of glucose uptake and metabolism in skeletal muscles [28]. Furthermore, the mechanisms by which P38 MAPK modulates PGC-1α expression are seem to require ATF2 [29,30]. Results in this study illustrated that the levels of phosphorylated ATF2 and p38MAPK in skeletal muscles were markedly increased by celastrol treatment. Thus, our results showed that celastrol could drive the expression of PGC-1α in skeletal muscles of diet-induced obese mice through the activation of p38 MAPK/ATF2 pathway.

Hepatic gluconeogenesis is pivotal for adaptation to fasting states, and its abnormal elevation is a major determinant of fasting hyperglycemia in diabetes [31]. PGC-1α is upregulated in several models of diabetes where gluconeogenesis is elevated, highlighting its importance in controlling blood glucose levels [32,33]. PGC-1α activates hepatic gluconeogenic gene expression, such as PEPCK and G6Pase [33,34]. In the present study, our results showed that administration of celastrol could inhibit PGC-1α levels in the liver, suggesting that PGC-1α is required for the consequent anti-hyperglycemic effect of celastrol. In addition, CREB is a key regulator of hepatic gluconeogenesis. CREB stimulates hepatic gluconeogenesis by increasing the expression of PGC-1α [34–36]. In the current study, we found that the reduction of hepatic p-CREB, brought on by treatment of celastrol, reduces expression of PGC-1α. Consequently, low level of PGC-1α in liver can suppress expression of PEPCK and G6Pase, and attenuate dysregulation of hepatic gluconeogenesis associated with the consumption of diet high in fat, thereby reducing hepatic glucose production. Therefore, we conclude that celastrol ameliorates gluconeogenic activity mainly through inhibition of CREB/PGC-1α signal pathway.

In conclusion, these results provide evidence in support of the central role of celastrol in regulating food intake and body weight by regulating GAL system. While further studies are needed to unravel the exact mechanism of actions of celastrol in inhibiting GAL system. In

addition to these direct anti-obesity activities, celastrol augmented the PGC-1α and GLUT4 expression in adipocytes and skeletal muscles to reduce insulin resistance through AKT and P38 MAPK activation. Celastrol also inhibited gluconeogenic activity through a CREB/PGC-1α pathway. This study contributes to our understanding of the anti-obesity and anti-diabetic role of celastrol, and provides a possibility of using celastrol to treat obesity and insulin resistance in clinic.

## Transparency document

The Transparency document associated with this article can be found, in online version.

## Acknowledgments

This work was supported by the National Health and Family Planning Commission of the People's Republic of China (Grant No. W201309) and the Natural Science Foundation of Jiangsu Province (No. BK20171319) and Science and technology project of Jiangsu Provincial Administration of Traditional Chinese Medicine (YB2015138) and Six Talent Peaks Project in Jiangsu Province (WSN-113) and Science and Technology Bureau of Taizhou (Grant No. TS201723) and Open Projects of Zoonosis Key Laboratory of Jiangsu Province (R1504).

.

## Conflict of interest

The authors declared no conflict of interest.

## References

[1] M.O. Goodarzi, Genetics of obesity: what genetic association studies have taught us about the biology of obesity and its complications, Lancet Diabetes Endocrinol. 6 (2018) 223–236.
[2] S.R. Chen, Y. Dai, J. Zhao, L. Lin, Y. Wang, Y.A. Wang, Mechanistic overview of triptolide and celastrol, natural products from Tripterygium wilfordii hook F, Front. Pharmacol. 9 (2018) 104.
[3] X. Ma, L. Xu, A.T. Alberobello, Celastrol protects against obesity and metabolic dysfunction through activation of a HSF1-PGC1α transcriptional axis, Cell Metab. 22 (2015) 695–708.
[4] Y. Zhang, C. Geng, X. Liu, M. Li, M. Gao, X. Liu, F. Fang, Y. Chang, Celastrol ameliorates liver metabolic damage caused by a high-fat diet through Sirt1, Mol. Metab. 6 (2016) 138–147.
[5] S.K. Choi, S. Park, S. Jang, H.H. Cho, S. Lee, S. You, S.H. Kim, H.S. Moon, Cascade regulation of PPARγ(2) and C/EBPα signaling pathways by celastrol impairs adipocyte differentiation and stimulates lipolysis in 3T3-L1 adipocytes, Metabolism 65 (2016) 646–654.
[6] J. Liu, J. Lee, M.A. Salazar Hernandez, R. Mazitschek, U. Ozcan, Treatment of obesity with celastrol, Cell 161 (2015) 999–1011.
[7] P. Fang, M. Yu, L. Guo, P. Bo, Z. Zhang, M. Shi, Galanin and its receptors: a novel strategy for appetite control and obesity therapy, Peptides 36 (2012) 331–339.
[8] G.Q. Chang, V. Gaysinskaya, O. Karatayev, S.F. Leibowitz, Maternal high-fat diet and fetal programming: increased proliferation of hypothalamic peptide producing neurons that increase risk for overeating and obesity, J. Neurosci. 28 (2008) 12107–12119.
[9] V.A. Gaysinskaya, O. Karatayev, G.Q. Chang, S.F. Leibowitz, Increased caloric intake after a high-fat preload: relation to circulating triglycerides and orexigenic peptides, Physiol. Behav. 91 (2007) 142–153.
[10] R. Yun, J.T. Dourmashkin, J. Hill, E.C. Gayles, S.K. Fried, Leibowitz SF. PVN galanin increases fat storage and promotes obesity by causing muscle to utilize carbohydrate more than fat, Peptides 26 (2005) 2265–2273.
[11] O. Karatayev, J. Baylan, S.F. Leibowitz, Increased intake of ethanol and dietary fat in galanin overexpressing mice, Alcohol 43 (2009) 571–580.
[12] O. Karatayev, J. Baylan, V. Weed, S. Chang, D. Wynick, S.F. Leibowitz, Galanin knockout mice show disturbances in ethanol consumption and expression of hypothalamic peptides that stimulate ethanol intake, Alcohol. Clin. Exp. Res. 34 (2010) 72–80.
[13] A.C. Adams, J.C. Clapham, D. Wynick, J.R. Speakman, Feeding behaviour in galanin knockout mice supports a role of galanin in fat intake and preference, J. Neuroendocrinol. 20 (2008) 199–206.
[14] M. Kiaei, K. Kipiani, S. Petri, J. Chen, N.Y. Calingasan, M.F. Beal, Celastrol blocks neuronal cell death and extends life in transgenic mouse model of amyotrophic lateral sclerosis, Neurodegener. Dis. 2 (2005) 246–254.
[15] A. Laque, S. Yu, E. Qualls-Creekmore, S. Gettys, C. Schwartzenburg, K. Bui, C. Rhodes, H.R. Berthoud, C.D. Morrison, B.K. Richards, H. Münzberg, Leptin modulates nutrient reward via inhibitory galanin action on orexin neurons, Mol. Metab. 4 (10) (2015) 706–717.
[16] T. Ohtaki, S. Kumano, Y. Ishibashi, K. Ogi, H. Matsui, M. Harada, C. Kitada, T. Kurokawa, H. Onda, M. Fujino, Isolation and cDNA cloning of a novel galanin-like peptide (GALP) from porcine hypothalamus, J. Biol. Chem. 274 (1999) 37041–37045.
[17] P. Fang, M. Yu, X. Gu, M. Shi, Y. Zhu, Z. Zhang, P. Bo, Circulating galanin and galanin like peptide concentrations are correlated with increased triglyceride concentration in obese patients, Clin. Chim. Acta 461 (2016) 126–129.
[18] J.E. Kim, M.H. Lee, D.H. Nam, Celastrol, an NF-κB inhibitor, improves insulin resistance and attenuates renal injury in db/db mice, PLoS One 8 (2013) e62068.
[19] M.H.A. Bakar, J.S. Tan, Improvement of mitochondrial function by celastrol in palmitate-treated C2C12 myotubes via activation of PI3K-Akt signaling pathway, Biomed. Pharmacother. 93 (2017) 903–912.
[20] D. Leto, A.R. Saltiel, Regulation of glucose transport by insulin: traffic control of GLUT4, Nat. Rev. Mol. Cell Biol. 13 (2012) 383–396.
[21] Z. Wu, P. Puigserver, U. Andersson, C. Zhang, G. Adelmant, V. Mootha, A. Troy, S. Cinti, B. Lowell, R.C. Scarpulla, B.M. Spiegelman, Mechanisms controlling mitochondrial biogenesis and respiration through the thermogenic coactivator PGC-1, Cell 98 (1999) 115–124.
[22] C.R. Benton, G.P. Holloway, X.X. Han, Y. Yoshida, L.A. Snook, J. Lally, J.F. Glatz, J.J. Luiken, A. Chabowski, A. Bonen, Increased levels of peroxisome proliferator-activated receptor gamma, coactivator 1 alpha (PGC-1alpha) improve lipid utilisation, insulin signalling and glucose transport in skeletal muscle of lean and insulin-resistant obese Zucker rats, Diabetologia 53 (2010) 2008–2019.
[23] L.F. Michael, Z. Wu, R.B. Cheatham, P. Puigserver, G. Adelmant, J.J. Lehman, D.P. Kelly, B.M. Spiegelman, Restoration of insulin-sensitive glucose transporter (GLUT4) gene expression in muscle cells by the transcriptional coactivator PGC-1, Proc. Natl. Acad. Sci. U. S. A. 98 (2001) 3820–3825.
[24] P. Puigserver, Z. Wu, C.W. Park, R. Graves, M. Wright, B.M. Spiegelman, A cold-inducible coactivator of nuclear receptors linked to adaptive thermogenesis, Cell 92 (6) (1998) 829–839.
[25] K. Sakamoto, G.D. Holman, Emerging role for AS160/TBC1D4 and TBC1D1 in the regulation of GLUT4 traffic, Am. J. Phys. 295 (2008) E29–E37.
[26] D. Samovski, X. Su, Y. Xu, N.A. Abumrad, P.D. Stahl, Insulin and AMPK regulate FA translocase/CD36 plasma membrane recruitment in cardiomyocytes via Rab GAP AS160 and Rab8a Rab GTPase, J. Lipid Res. 53 (2012) 709–717.
[27] P.J. Fernandez-Marcos, J. Auwerx, Regulation of PGC-1α, a nodal regulator of mitochondrial biogenesis, Am. J. Clin. Nutr. 93 (2011) 884S–890S.
[28] D. Konrad, R. Somwar, G. Sweeney, K. Yaworsky, M. Hayashi, T. Ramlal, A. Klip, The antihyperglycemic drug alpha-lipoic acid stimulates glucose uptake via both GLUT4translocation and GLUT4 activation: potential role of p38 mitogen-activated protein kinase in GLUT4 activation, Diabetes 50 (2001) 1464–1471.
[29] T. Akimoto, S.C. Pohnert, P. Li, M. Zhang, C. Gumbs, P.B. Rosenberg, R.S. Williams, Z. Yan, Exercise stimulates Pgc-1alpha transcription in skeletal muscle through activation of the p38 MAPK pathway, J. Biol. Chem. 280 (2005) 19587–19593.
[30] H.J. Jeong, H.J. Lee, T.A. Vuong, K.S. Choi, D. Choi, S.H. Koo, S.C. Cho, H. Cho, J.S. Kang, Prmt7 deficiency causes reduced skeletal muscle oxidative metabolism and age-related obesity, Diabetes 65 (2016) 1868–1882.
[31] A.K. Rines, K. Sharabi, C.D. Tavares, P. Puigserver, Targeting hepatic glucose metabolism in the treatment of type 2 diabetes, Nat. Rev. Drug Discov. 15 (2016) 786–804.
[32] K. Sharabi, H. Lin, C.D.J. Tavares, J.E. Dominy, J.P. Camporez, R.J. Perry, R. Schilling, A.K. Rines, J. Lee, M. Hickey, M. Bennion, M. Palmer, P.P. Nag, J.A. Bittker, J. Perez, M.P. Jedrychowski, U. Ozcan, S.P. Gygi, T.M. Kamenecka, G.I. Shulman, S.L. Schreiber, P.R. Griffin, P. Puigserver, Selective chemical inhibition of PGC-1α gluconeogenic activity ameliorates type 2 diabetes, Cell 169 (2017) 148–160.
[33] J.C. Yoon, P. Puigserver, G. Chen, J. Donovan, Z. Wu, J. Rhee, G. Adelmant, J. Stafford, C.R. Kahn, D.K. Granner, C.B. Newgard, B.M. Spiegelman, Control of hepatic gluconeogenesis through the transcriptional coactivator PGC-1, Nature 413 (2001) 131–138.
[34] J.T. Rodgers, C. Lerin, W. Haas, S.P. Gygi, B.M. Spiegelman, P. Puigserver, Nutrient control of glucose homeostasis through a complex of PGC-1alpha and SIRT1, Nature 434 (2005) 113–118.
[35] S. Herzig, F. Long, U.S. Jhala, S. Hedrick, R. Quinn, A. Bauer, D. Rudolph, G. Schutz, C. Yoon, P. Puigserver, B. Spiegelman, M. Montminy, CREB regulates hepatic gluconeogenesis through the coactivator PGC-1, Nature 413 (2001) 179–183.
[36] S.H. Koo, L. Flechner, L. Qi, X. Zhang, R.A. Screaton, S. Jeffries, S. Hedrick, W. Xu, F. Boussouar, P. Brindle, H. Takemori, M. Montminy, The CREB coactivator TORC2 is a key regulator of fasting glucose metabolism, Nature 437 (2005) 1109–1111.